

# **Infrared thermography: a powerful tool to characterize the thermomechanical and fatigue properties of short glass fiber reinforced thermoplastics structural samples**

**V. Le Saux<sup>1</sup>, Y. Marco<sup>1</sup>, A. Launay<sup>2</sup>, L. Jégou<sup>3</sup> and S. Calloch<sup>1</sup>**

<sup>1</sup> Européenne de Bretagne, ENSTA Bretagne - Laboratoire Brestois de Mécanique et des Systèmes EA 4325. 2 rue François Verny, F-29806 Brest Cedex 9, France.  
E-mail : vincent.le\_saux@ensta-bretagne.fr

<sup>2</sup> PSA Peugeot Citroën, Route de Gisy, F-78943 Vélizy-Villacoublay cedex, France.  
E-mail : antoine.launay@mps.com

<sup>3</sup> Université Européenne de Bretagne, IUT Saint-Brieuc. Rue Henry Wallon, F-22000 Saint-Brieuc, France.  
E-mail : loic.jegou@univ-rennes1.fr

## **ABSTRACT.**

*Components made of short glass fiber reinforced thermoplastics are increasingly used in the automotive industry in order to reduce the price and weight of the vehicle. These components are frequently submitted to fatigue loadings during their service conditions. Therefore, a good conception towards the fatigue phenomenon is mandatory. One preliminary need is to model correctly the non linear behavior of such material, which is clearly not an easy task due to the numerous dissipation mechanisms involved and the strong anisotropy induced by the injection process. In this study, we present some results on injected samples with a specific geometrical accident leading to a stress concentration factor  $K_t=2.5$ . A specific thermomechanical characterization is done using an infrared camera. Several key informations can be extracted from these experimental data: temperature variations, heat sources, crack initiation localization, crack propagation (detection of the crack vicinity), etc. These data are then compared to numerical simulations involving the simulation of the injection step and finite element analysis using an anisotropic elasto-viscoplastic model. The heat sources obtained with the model are compared the experimental ones. A very good agreement between the experimental data and the numerical ones is found which illustrate the relevancy of the model to capture some key thermomechanical properties of these materials, which is obviously a key element in the fatigue life prediction.*

## **INTRODUCTION**

In order to reduce its CO<sub>2</sub> emission and fuel consumption, the automotive industry wishes to substitute heavy metallic parts by lightweight composites structures. Short glass fibers reinforced (SGFR) thermoplastics are appropriate candidates because they

combine high stiffness and a very good productivity induced by the costless injection molding process.

These materials have been used for long in the automotive industry for components that do not undergo very high cyclic thermomechanical loadings. They are nowadays increasingly used for structural applications such as engine mounts or clutch pedal, which are submitted to complex cyclic loadings with temperature and humidity variations. Therefore, for most of the carmakers, the design of plastic parts against fatigue failure has become a serious issue these last few years. They now have to guarantee the lifetime of these plastic components which is clearly a very complex problem due to the nature of these materials that exhibit a highly anisotropic non-linear behavior with a strong dependency of the thermo-hygro-mechanical behavior to the environment [1].

The modeling of the cyclic behavior of such materials still remains an open issue, as well as defining an efficient fatigue criterion. The objective of this paper is to show that infrared measurements under cyclic loading can bring very useful data to investigate fatigue behavior and can be an appropriate tool to validate both numerical simulation and fatigue criterion.

This paper is divided into two main parts. In the first one, the experimental and numerical tools are shortly described. Then, some experimental data are presented and finally, a comparison to numerical prediction is performed.

## **EXPERIMENTAL AND NUMERICAL TOOLS**

### ***Infrared camera and testing machine***

All the experimental data have been obtained on an INSTRON hydraulic testing machine equipped with a 100kN load cell. All the tests have been load controlled and were conducted at 1Hz in order to limit as much as possible the heat build-up (the coupling of the thermomechanical properties to the temperature can therefore be neglected).

The infrared measurements were achieved with a FLIR SC7600BB camera equipped with a 50mm and G1 objectives. The FPA is 640\*512 pixels and the pitch is 15 $\mu$ m. In order to get the best accuracy possible, a homemade calibration procedure was developed (pixelwise calibration integrating the effects of the camera housing temperature) and permits a thermal resolution of 10mK under differential measurements.

### ***Samples***

We focused in this study on a notch fatigue sample made of polyamide 66 reinforced with 35% of glass short fibers (in mass). The stress concentration factor induced by the hole is 2.5. Even if this geometry seems quite simple, the orientation distribution is disturbed by the geometrical accident and induces a complex orientation and thus a strong anisotropy (highlighted by figure 2).

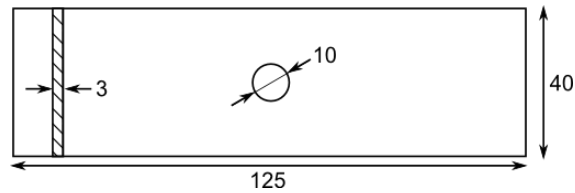


Figure 1. Geometry of the specimen. Dimensions are given in mm.

### ***Heat build-up test***

Heat build-up tests are becoming more or more used by the fatigue community. They are the basis of a rapid characterization for various types of materials ranging from metallics [2] or rubber-like materials [3] to short fibers composites [4]. The principle is quite simple and consists in submitting a sample to cyclic tests of increasing stress (or strain) amplitude. The temperature of the surface sample is recorded and a heat build-up curve is then built relating the stress (or strain) amplitude to the stabilized temperature variation or to the dissipated energy. This curve is usually used to identify an energetic criterion for fatigue and to plot a Wöhler curve. Here, the curve will be used to compare the experimental results to the numerical ones. The use of this curve for fatigue purpose will be discussed in a companion paper presented by Marco *et al.*

### ***Numerical tools***

The aim of the numerical tools is to simulate the cyclic mechanical responses of this sample when submitted to various loading. Due to the complex microstructure of these materials, the numerical chain is composed of several main steps. The basic idea of the numerical tool is presented on figure 1 and consists of 3 main steps: first, an injection simulation is performed using the Moldflow<sup>®</sup> software in order to get the fiber orientation distribution through the second and fourth order moments. In most cases, the meshes for the injection simulation and the mechanical simulations are different. Therefore, an interpolation of the orientation tensors on the mechanical mesh is needed. This operation is performed using the mapping software Digimat-MAP<sup>®</sup>. Finally, the mechanical simulation using the Abaqus<sup>®</sup> finite element code is performed. For this latter part, we used the specific constitutive behaviour suggested by Launay *et al.* [5] that takes into account the injection induced anisotropy (thanks to the orientation tensors defined at each gauss point of the FE mesh after the interpolation step), short-term and long-term viscoelasticity, viscoplasticity, cyclic softening and the influence of the environment (temperature and humidity) through a dependency of the constitutive parameter to the temperature gap  $T-T_g$  [1]. This model has been implemented thanks to a UMAT user subroutine written in FORTRAN. As the model is written in a thermodynamical framework, it is also possible to evaluate the global energy dissipated, as well as the dissipated energy by each non-elastic phenomenon. In this article, only the global dissipated energy will be analysed.

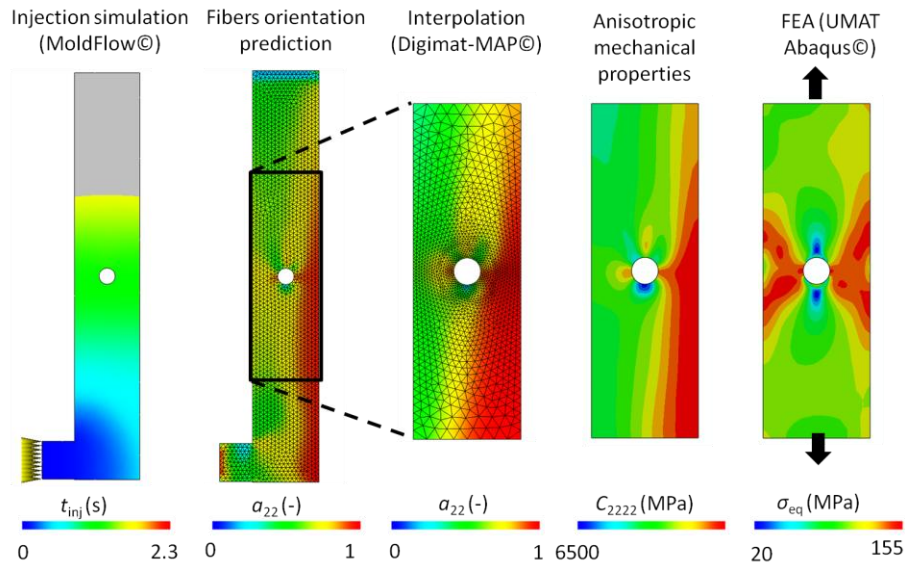


Figure 1. Global representation of the numerical procedure used to estimate the mechanical behaviour.

## RESULTS

### *Analysis of the thermal mappings: application to the propagation of a fatigue crack*

Due to the bad thermal conductivity of these materials, it is possible to analyze the localisation of the heat sources on the temperature mapping. Figure 3 shows for exemple several temperature mappings obtained after various numbers of cycles for a nominal stress amplitude of 44MPa (the last point of the heat build-up experiment). It should be noticed that the classical butterfly wings are clearly visible, and a disymetry of these wings is observed due to the injection molded induced anisotropy. Moreover, a hot spot on the left side of the hole at 3mm distance to the surface is noticed on figure 3a. There is a clear shift of this spot on figure 3b with an increase of the phenomenom intensity. On figure 3c, the spot is clearly highlighted and the temperature localization is more important.

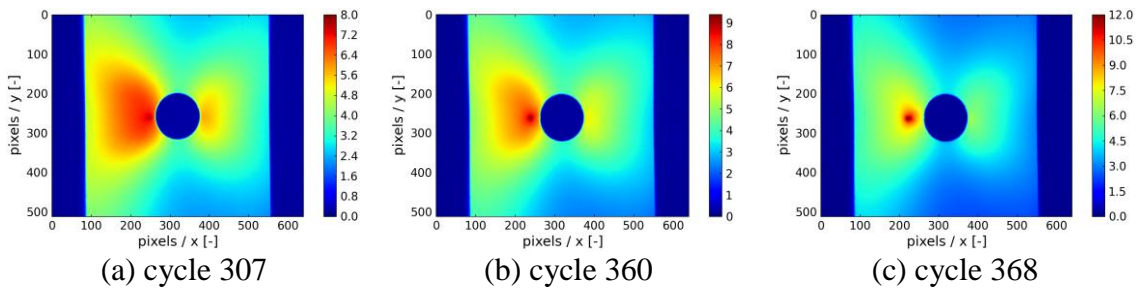


Figure 3. Evolution of the crack vicinity during the fatigue test. The mapping shown are differential temperature mapping.

This localization could be emphasized by analyzing the temperature profil along a line (figure 4). The maximum temperature variation has been followed for various numbers of cycles and the results are presented on figure 5. We can point out an initiation that is not located on the free edge of the hole, which is not consistent with the location of the maximum stress and strain.

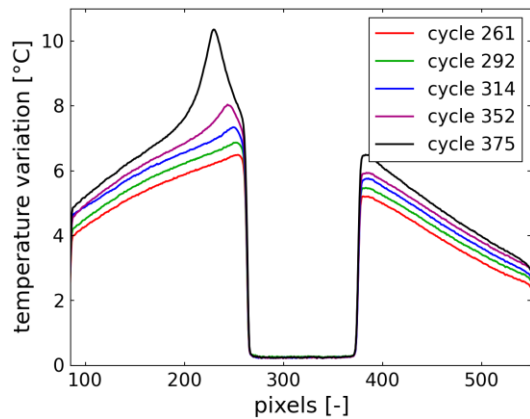


Figure 4. Evolution of the temperature profile.

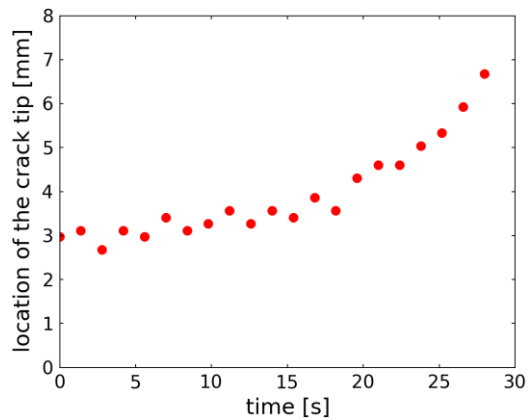


Figure 5. Evolution of the crack vicinity before the failure.

To check that the interpretation of these thermal measurements is consistent with the damage scenario that leads to the final fracture of the sample, we have performed some SEM observations of the fracture surface at specific locations (around the zone we have identified with the thermal measurements and far from this zone). These results are presented on figure 6. These SEM data clearly point out different damage mechanisms, which validates the interpretation of the thermal data.

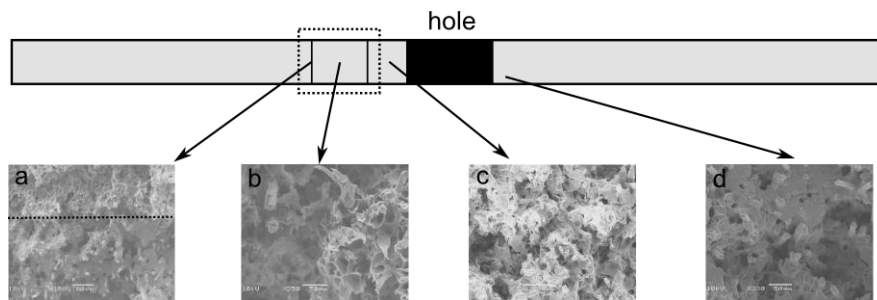


Figure 6. SEM observation of the fracture surface.

***Experimental evaluation of the thermal heat sources***

Even if the analysis of the thermal fields clearly brings very useful information, temperature remains only the consequence of the internal dissipation and is clearly not an intrinsic property of the material. It could be more interesting to try to get back to the heat sources, *i.e.* the terms that are responsible for these temperature variations. Temperature and heat sources are related through the heat equation [7]:

$$\rho c \frac{\partial T}{\partial t} + \lambda \Delta T = \Delta_{\text{int}} + r + \rho c \frac{\partial^2 \psi}{\partial V_k \partial T} : \dot{V}_k + \rho c \frac{\partial^2 \psi}{\partial \varepsilon_e \partial T} : \dot{\varepsilon}_e \quad (1)$$

Under some classical assumptions [4], it is possible to simplify this equation:

$$\rho c \frac{\partial \theta}{\partial t} + \lambda \Delta \theta = \Delta_{\text{int}} \quad (2)$$

where the  $\theta$  represents the temperature variation. Two strategies can be applied to estimate the heat sources. The first one consists in considering the temporal and spatial temperature variation gradients to solve the inverse problem, as classically performed in the literature [2,6]. This solution is clearly not an easy task here due to the complex geometry of the sample. A complex finite element approach is here (correct application of the thermal boundary conditions, etc). The second one takes advantage of the low thermal conductivity of these materials and consists in considering the very first temporal step of equation (2). If we consider  $t \rightarrow t_0$ , the spatial diffusion can be neglected and equation 2 simply becomes:

$$\rho c \frac{\partial \theta}{\partial t} \Big|_{t \rightarrow 0} = \Delta_{\text{int}} \quad (3)$$

which can be approximated experimentally according to a finite difference evaluation:

$$\rho c \left( \frac{\theta_2 - \theta_1}{t_2 - t_1} \right) = \Delta_{\text{int}} \quad (4)$$

From a theoretical point of view, the approach is clearly appealing. The difficulties rather come from the experimental point of view in that case because very small temperature variations are expected. Moreover, depending on the way to evaluate the left side of equation 4, *i.e.* depending on the image 1 and 2, the results can be “sensibly” different as illustrated on figure 7 for IR image.

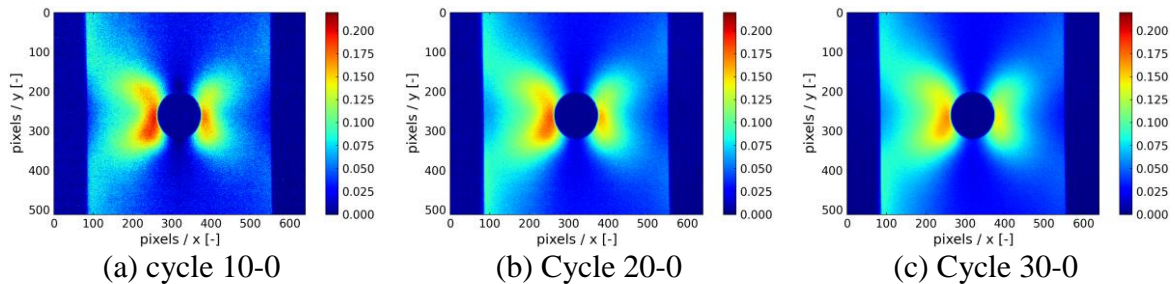


Figure 7. Influence of the way to evaluate the heat sources. Units:  $\text{mJ}/\text{mm}^3$ .

In the following, all the heat sources quantities have been evaluated by considering cycle 0 subtracted from cycle 2.

### ***Comparison between the experimental heat sources and numerical ones***

We discuss in that section the comparison between the heat sources mapping estimated experimentally using the strategy detailed previously and the numerical ones computed

using the numerical chain detailed in the first section. The identification of the numerical model is not discussed in this paper. Please refer to Launay *et al.* [6] for details.

Figure 8 presents a comparison between the predicted and the evaluated heat sources mappings. The agreement is quite good. In both cases, asymmetrical butterfly wings are noticed due to the anisotropy.

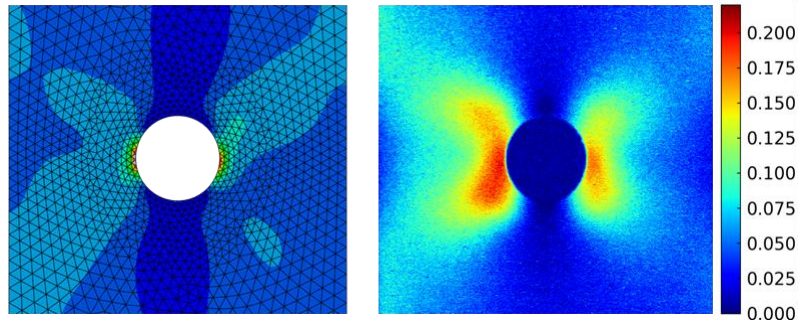


Figure 8. Comparison between the numerical and experimental dissipated energy mappings. Units:  $\text{mJ}/\text{mm}^3$ .

Even if the graphical comparison of the heat source mapping is very interesting, it remains a qualitative analysis. To bring quantitative data, we have performed a mean operation in small zones. The first one is at a given distance from the free edge and has been chosen here because the dissipation is maximal in that location. The second one is more in the core of the sample and has been chosen in that location we wanted to check the capability of the model to capture the gradient effects. Here, the G1 objective is used in order to improve the spatial resolution of the analysed zones (dimensions of  $5 \times 7 \text{mm}$ ).

The results are given in figure 8. Globally, a very good agreement is noticed for the zone 1. The model correctly captures the non linear heat build-up curve. Dealing with the zone 2, we can observe an underestimation of the dissipated energy beyond 30MPa of stress amplitude which could unfortunately leads to a non conservative lifetime prediction if we consider a fatigue criterion based on a dissipation approach. These differences can be explained by a bad estimation of the fiber orientation in that location and clearly highlight one drawback of a fully numerical approach.

## CONCLUSION

We have presented in this communication some experimental and numerical results based on the analysis of thermal measurements of short glass fibers reinforced (SGFR) thermoplastics when submitted to cyclic loadings. Two main points can be pointed out:

1. the thermal fields are very rich, in particular in the case of fatigue crack propagation. The crack induces a strong stress concentration in its vicinity leading to an important dissipated energy and thus temperature rise. Due to the

low thermal conductivity of these materials, the analysis of the thermal mapping allows us to follow the crack.

2. The analysis of thermal fields can lead to a dissipated energy mapping, therefore a fatigue lifetime mapping considering an energetic fatigue life criterion. Moreover, these data can be very useful for the validation of constitutive model and fatigue criterion. Moreover, using digital image correlation and infrared measurements, it is possible to get access to the heat sources field and the strain fields. By analyzing these data, an access to the stress field seems possible, which could be very interesting.

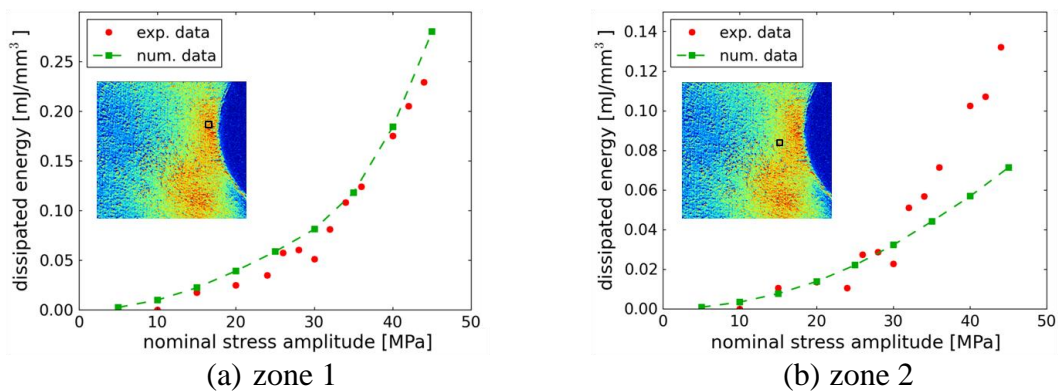


Figure 9. Mean dissipated energy plotted as a function of the nominal stress amplitude.

## REFERENCES

1. Launay, A., Marco, Y., Maitournam, M.H., Raoult, I. (2013) *Mechanics of Materials* **56**, 1-10.
2. Doudard, C., Calloch, S., Hild, F, Roux, S (2010), *Mechanics of Materials* **42**, 55-62.
3. Le Saux, V., Marco, Y., Calloch, S., Doudard, C., Charrier, P (2010), *International Journal of Fatigue* **32**, 1582-1590.
4. Jegou, L., Marco, Y., Le Saux, V., Calloch, S. (2012), *International Journal of Fatigue* **47**, 259-267.
5. Launay, A., Maitournam, M.H., Marco, Y., Raoult, I., Szmytka, F. (2011), *International Journal of Plasticity* **27**, 1267-1293.
6. Chrysochoos, A., Louche, H (2000), *International Journal of Engineering Science* **38**, 1759-1788.
7. Lemaitre, J., Chaboche, J.L. *Mécanique des Matériaux Solides*, Dunod, 1990.